

Approximations for the direct correlation function in multicomponent molecular fluids

A. Chamoux and A. Perera

Citation: *J. Chem. Phys.* **104**, 1493 (1996); doi: 10.1063/1.470915

View online: <http://dx.doi.org/10.1063/1.470915>

View Table of Contents: <http://jcp.aip.org/resource/1/JCPSA6/v104/i4>

Published by the [American Institute of Physics](#).

Additional information on J. Chem. Phys.

Journal Homepage: <http://jcp.aip.org/>

Journal Information: http://jcp.aip.org/about/about_the_journal

Top downloads: http://jcp.aip.org/features/most_downloaded

Information for Authors: <http://jcp.aip.org/authors>

ADVERTISEMENT



Goodfellow
metals • ceramics • polymers • composites
70,000 products
450 different materials
small quantities fast
www.goodfellowusa.com

Approximations for the direct correlation function in multicomponent molecular fluids

A. Chamoux and A. Perera

Laboratoire de Physique Théorique des Liquides,^{a)} Université Pierre et Marie Curie, 4, place Jussieu, 75252 Paris Cedex 05, France

(Received 10 July 1995; accepted 28 September 1995)

Analytical approximations for the pair direct correlation function (DCF) of molecular fluids and their mixtures are derived within the frame of a new formalism based on weighted density functional methods which represents a generalization of Rosenfeld theory for hard spheres mixtures [J. Chem. Phys. **89**, 4271 (1988)]. These approximations rest upon the geometrical properties of individual molecules such as the volume, the surface, and the mean radius. They are Percus–Yevick (PY) like in nature and reduce to the analytical PY solution for DCF in the hard sphere case. By construction the approximations incorporate several interesting features: They yield the Mayer function in the low density limit as expected, and they are anisotropic at zero separation as well as at contact. In addition they predict an orientational instability of the isotropic phase with respect to the nematic phase, a feature that is absent from the Percus–Yevick theory. Comparisons are made with the Percus–Yevick numerical results for the DCF for various convex hard bodies such as hard ellipsoids of revolutions (prolate and oblate), prolate spherocylinders, cutspheres, and generally the agreement is very good for a large range of liquid densities. Analytical expressions for the virial and compressibility routes for the pressures are also given. The results obtained for a large varieties of convex bodies are in very good agreement with corresponding numerical Percus–Yevick results. These approximations can be generalized to inhomogeneous systems in a straightforward manner. © 1996 American Institute of Physics. [S0021-9606(96)51601-6]

I. INTRODUCTION

The pair direct correlation function (DCF) is an essential ingredient in the theory of fluids, together with the pair distribution function to which it is linked through the Ornstein Zernike equation.¹

The Percus–Yevick analytical solution for the pair DCF of hard sphere has induced considerable theoretical progress in the study of simple liquids. There is unfortunately no such solution available for hard nonspherical particles.

Yet, it is clear that hard core molecular models play an important role in understanding complex liquids, such as liquid crystals. The recent results in computer simulations have exhibited the various liquid crystalline phase behavior these simple models can show.² The development of theoretical background for a true microscopic approach to complex fluids can profit to a great extent from a reliable analytical approximation for the pair DCF.

Density functional theories (DFT) in general provide a suitable framework for studying all the various liquid crystal phases of nonspherical particles in particular.^{2,3} The pair DCF is precisely the most important ingredient of such theories. At this point, one must admit that a precise knowledge of the DCF is unnecessary in order to obtain results that are in reasonably good agreement with computer simulations, at least in the framework of DFT, and as far as structural properties are not concerned.

For example, a simple approximation for the DCF which decouples the radial part (treated hence with the hard sphere

PY DCF) from the angular part (treated at Onsager level of approximation) leads to one of the most accurate version of such theories, as formulated by Baus and co-workers,⁴ and which predicts very satisfactorily the isotropic to nematic phase transition of the hard ellipsoids systems, as well as the equation of state (EOS) in both phases. The DFT theory of Somoza and Tarazona⁵ has also a very good predictive power as compared to the simulations although no explicit approximation for the DCF is involved.

The main reason for this success is that the excess free energies of such theories, even though truncated at second order in density expansion, incorporates higher order correlations through the pair DCF by some rescaling (or weighting) of the densities. These weighted density functional theories (WDFT) are in general more powerful than simple second order DFT.⁶

The Pynn approximation⁷ which relies on the PY analytical expression of the hard sphere DCF by using angle dependent intermolecular separation, has been also tested successfully in the case of the nematic–smectic *A*-solid transition for parallel hard spherocylinders.^{8,9} Whereas this approximation has been tested to be quite reliable for small elongations,¹⁰ its validity for arbitrary elongation is not clear. It has several well known drawbacks: It does not give the Mayer function $f(1,2)=\exp(-\phi(1,2)/k_B T)-1$ in the zero density limit as it should; furthermore it is isotropic at $r=0$ and at contact, which is unphysical. One of the intriguing features of these theories is that the DCF of the reduced symmetry phase is unknown, and thus this function is somehow tailored on its isotropic counter part. For this reason it

^{a)}Unité associée au C.N.R.S.

would be of fair interest to know how to calculate the correct features of the DCF.

A recent fruitful approach by Rickayzen and co-workers¹¹ has put forward an analytic expression for the pair DCF which is restricted to particular angles. This restriction permits the full analyticity of the expressions and works quite well in describing the density profile of hard ellipsoids in pores. However the validity of such approach to the bulk fluid is still unclear.

In a remarkable paper,¹² Rosenfeld has introduced a general weighted density functional theory (WDFT) that is applicable in particular to hard convex bodies and which gives a geometrical interpretation of the hard sphere DCF for the PY approximation. For the hard sphere system, this formalism reduces to the PY approximation through a convolution of weights which depends only on the individual molecular geometry. This perspective seems extremely appealing since there is no obvious physical interpretation of the DCF as compared to the pair distribution function, and as a consequence of this there is no way of “measuring” directly the DCF using computer simulation methods, for example (as opposed to the pair correlation function). This formalism, and some variants of it^{13,14} has been studied extensively for the hard sphere system. One of the appealing features is that it allows systematic derivations of higher order DCF and straightforward extensions to inhomogeneous systems. Hence, it would be interesting to examine applications to the case of hard nonspherical bodies.

However, as we show here, this formalism when strictly applied to hard anisotropic particles leads to an *isotropic* DCF at $k=0$, k being the inverse Fourier wavelength. In addition, it does not give the correct Mayer function in the zero density limit. The major conclusion drawn here is that the Mayer function in particular and thus the DCF in general, cannot be written as a convolution of weights. A similar conclusion was obtained very recently by Rosenfeld by geometrical considerations on convex bodies.¹⁵

We propose some simple approximations that correct these deficiencies without loss of generality in the formalism. The rest of the paper is as follows. In the next section we present the weighted density formalism for mixtures of non-spherical hard cores, and examine the consequences concerning the Mayer function. The corrective approximations are also presented for the general case of mixtures of convex molecules. Section III shows the results for the case of prolate and oblate hard ellipsoids of revolution as well as for prolate spherocylinders and cutspheres, and for several aspect ratios. The conclusions are presented in Sec. IV.

II. THEORY

A. The weighted density functional theory formalism

The general version of this theory for hard spheres mixtures has been given by Rosenfeld^{12,13} which is extended below in a straightforward manner in order to incorporate angle dependent variables.

The starting point is to write the excess free energy density in terms of weighted densities $n_\alpha(1)$ introducing thus a

set of weights containing the geometrical information concerning each molecular species i of an N -component system, $w_i^{(\alpha)}(1) = w_i^{(\alpha)}(\mathbf{r}, \mathbf{\Omega})$ which depends on the position \mathbf{r} of the center of mass and the orientation $\mathbf{\Omega}$ of each particle with respect to the lab fixed frame.

The excess free energy is then expressed formally as

$$\beta F^{\text{ex}}[\rho] = \int d1 \Phi(\{n_\alpha(1)\}) \quad (1)$$

with the weighted densities

$$n_\alpha(1) = \sum_i \int d2 \rho(2) w_i^{(\alpha)}(1, 2), \quad (2)$$

where $\rho(1)$ is the number density of the inhomogeneous system. In this expression the notation $w_i^{(\alpha)}(1, 2)$ indicates that the weight variables are measured in the frame fixed by the position and orientation of particle 1.

As a consequence of Eq. (1) the *homogeneous* n -body direct correlation functions are written as a convolution product

$$\begin{aligned} -C_{i_1 \dots i_n}^{(n)}(1, \dots, n) &= \frac{\delta^{(n)} \beta F^{\text{ex}}}{\delta \rho(1) \dots \delta \rho(n)} \\ &= \sum_{\alpha_1, \dots, \alpha_n} \Phi_{\alpha_1 \dots \alpha_n} w_{i_1}^{(\alpha_1)}(1) \star \dots \star w_{i_n}^{(\alpha_n)}(n), \end{aligned} \quad (3)$$

where we have noted the multiple partial derivative as

$$\Phi_{\alpha_1 \dots \alpha_n} = \frac{\partial^{(n)} \Phi}{\partial \bar{n}_{\alpha_1} \dots \partial \bar{n}_{\alpha_n}} \quad (4)$$

and \star denotes a convolution product. In the homogeneous case the free energy density Φ depends only on the variables $\bar{n}_\alpha = \xi_\alpha = \rho \tilde{w}_i^{(\alpha)}(k=0)$ as can be seen from Eq. (2), and where the tilde indicates a Fourier–Hankel transform. The nice separation between density dependent factors and spatial variables dependent ones makes the expression for the DCF in Eq. (3) very attractive. Another positive aspect is that the contribution from different species appears explicitly only through the convolution of weight functions, the density dependent prefactor being the same for any combination of the i_j factors. In order to go any further, an expression for the free energy density must be provided, and the weights and their number must be specified explicitly.

Concerning the free energy density, the simplest available expression is the scaled particle theory (SPT)¹⁶ expression for the PY excess free energy density which is expressed solely in terms of the following set of the four SPT variables $\{\xi_\alpha = \rho R_\alpha\}$ ($\alpha=0,1,2,3$), related to the geometrical properties of the molecules: $R_3=V$, $R_2=S$, $R_1=R_m$ and $R_0=1$, with V, S, R_m being, respectively, the volume, surface and mean radius of the convex object representing the molecule. The SPT free energy reads¹⁶

$$\Phi^{\text{PY-C}} = -\xi_0 \ln(1 - \xi_3) + \frac{\xi_1 \xi_2}{1 - \xi_3} + \frac{1}{24\pi} \frac{\xi_2^3}{(1 - \xi_3)^2}. \quad (5)$$

Strictly speaking the geometrical dependence in the variables V, S, R_m is a feature of convex bodies only. In particular, the second virial coefficient can be expressed entirely in terms of these variables only.¹⁷ However, this limitation can be bypassed in approximate theories, and eventually extended to nonconvex bodies such as molecules made of fused hard spheres.¹⁸

Concerning the weights, the method chosen by Rosenfeld¹³ is to introduce an arbitrary number of weights, including vectorial ones, by using some considerations on the expression of the free energy in the low density limit. This is equivalent to identifying the correct pair DCF in the same limit as the Mayer function. A second approach has been taken by Kierlik and Rosinberg¹⁴ who choose the hard sphere PY-DCF as reference for the pair DCF. In that way they are able to compute the weights rigorously, at the PY level. Both methods recover the same Percus–Yevick DCF of the hard spheres mixtures, and they also yield the same free energy,¹⁹ with a computational advantage to the second method which gives four unique weights as compared to the six given by the first one. This difference is particularly important when it comes to computing the higher order DCFs, where the rapid increase in the number of convolution terms makes the calculations laborious. The second approach cannot be used for molecular systems, as no analytical solutions are available for the pair DCF. Reconsidering then the first method, in view of the general expression (3) it is interesting to ask whether or not it can yield the Mayer function for the pair DCF, in the low density limit. Unfortunately, the answer is no, as is shown below. This failure is not limited to the pair DCF, and intimately stems from the fact that the weights are isotropic in the zero inverse wavelength limit $k=0$.

As mentioned in the beginning of this section, the weights are based on individual geometrical properties of the molecules. In general such weights can be expanded in a set of rotational invariants.²⁰ The most general expansion reads

$$w_i^{(\alpha)}(\mathbf{r}, \mathbf{\Omega}) = \sum_{m\mu} w_i^{(\alpha)m\mu}(r) \Phi_{\mu 0}^{m0m}(\mathbf{\Omega}, 0, \hat{r}), \quad (6)$$

where $\hat{r} = \mathbf{r}/|\mathbf{r}|$ is a unitary vector and where the $\Phi_{\mu\nu}^{mnl}(12)$ are defined as

$$\begin{aligned} \Phi_{\mu\nu}^{mnl}(12) &= f^{mnl} \sum_{\mu' \nu' \lambda} \begin{pmatrix} m & n & l \\ \mu' & \nu' & \lambda \end{pmatrix} \\ &\times R_{\mu' \mu}^m(\mathbf{\Omega}_1) R_{\nu' \nu}^n(\mathbf{\Omega}_2) R_{\lambda 0}^l(\hat{r}), \end{aligned} \quad (7)$$

where the $R_{\mu' \mu}^m(\mathbf{\Omega}_1)$ denotes the Wigner elements, and the symbol with brackets is a 3- j symbol. Taking the Fourier transform of $w_i^{(\alpha)}(\mathbf{r}, \mathbf{\Omega})$ we get²⁰

$$\tilde{w}_i^{(\alpha)}(\mathbf{k}, \mathbf{\Omega}) = \sum_{m\mu} \tilde{w}_i^{(\alpha)m\mu}(k) \Phi_{\mu 0}^{m0m}(\mathbf{\Omega}, 0, \hat{k}), \quad (8)$$

where the Fourier–Hankel coefficients are defined by

$$\tilde{w}_i^{(\alpha)m\mu}(k) = 4\pi(-i)^m \int_0^L dr r^2 w_i^{(\alpha)m\mu}(r) j_m(kr). \quad (9)$$

The upper bound of the integral is not ∞ but some finite length dependent on the geometry of the particle (usually the aspect ratio of the hard body). Now, taking the limit $k=0$ and using the properties of spherical Bessel function²¹ $j_m(x) \rightarrow x^m$ when $x \rightarrow 0$ we see that

$$\tilde{w}_i^{(\alpha)m\mu}(k=0) = 0 \quad m \neq 0. \quad (10)$$

The invariant expansion for the n -DCF, from Eq. (3), involves expanding a n -product of invariants. This product can be cast into a sum over single invariants by using the expansion of single Wigner elements.^{22,23} For the pair DCF such expansion reads

$$\Phi_{\mu 0}^{m0m}(\mathbf{\Omega}_1, \mathbf{k}) \Phi_{\nu 0}^{n0n}(\mathbf{\Omega}_2, \mathbf{k}) = \sum_l P_{\mu\nu}^{mnl} \Phi_{\mu\nu}^{mnl}(\mathbf{\Omega}_1, \mathbf{\Omega}_2, \mathbf{k}), \quad (11)$$

where the coefficient $P_{\mu\nu}^{mnl}$ depends on *all* indices in the expression above, and whose explicit expression can be obtained from Eq. (7) by standard manipulation of the 3- j symbols.^{22,24} In particular,

$$P_{00}^{mnl} = \frac{f^{m0m} f^{n0n}}{f^{mnl}} \frac{(2l+1)}{\sqrt{(2m+1)(2n+1)}} \begin{pmatrix} m & n & l \\ 0 & 0 & 0 \end{pmatrix}. \quad (12)$$

The final expression for the pair DCF in Fourier space is then

$$\tilde{C}_{ij}(1,2) = \sum_{\substack{m,n,l \\ \mu,\nu}} \tilde{C}_{\mu\nu;ij}^{mnl}(k) \Phi_{\mu\nu}^{mnl}(12), \quad (13)$$

where

$$\tilde{C}_{\mu\nu;ij}^{mnl}(k) = \sum_{\alpha,\beta} \Phi_{\alpha,\beta} P_{\mu\nu}^{mnl} \tilde{w}_i^{(\alpha)m\mu}(k) \tilde{w}_j^{(\beta)n\nu}(k). \quad (14)$$

From Eq. (10) we see that the convolution approximation leads to

$$\tilde{C}_{\mu\nu;ij}^{mnl}(k=0) = 0, \quad m, n \neq 0. \quad (15)$$

The isotropy of this DCF at $k=0$ is certainly incorrect, since in the low density limit it is different from the behavior of the Mayer function. More importantly this approximation cannot predict the instability of the isotropic phase for very elongated particles as the inverse Kerr constant⁶ $\Delta_2 = 1 - \rho \tilde{C}_{00}^{220}(k=0)$ is always unity here.

From Onsager²⁵ it is well known that in the $k=0$ limit, the Mayer function for very elongated cylinders is a function of the sine of the relative orientation of two molecules, and thus is anisotropic. The above approximation, despite its very appealing decoupling of the density and spatial variables is incorrect even at the Onsager level of approximation.

In order to keep the approximation correct at low density level it is important to incorporate the Mayer function in an ad hoc manner into the convolution approximation. There are different ways of doing this, as we now proceed to show.

B. Approximations for the pair DCF

Although one can introduce both scalar and vectorial weights¹³ we prefer to follow closely the approach of Kierlik and Rosinberg¹⁴ who introduce scalar weights. For the par-

ticular case of hard spheres both cases have been shown to be exactly equivalent.¹⁹ The weights that are introduced by these authors are the followings: A volume weight $H(|\mathbf{r}-\mathbf{R}_i|)$ where H is the Heaviside function and R_i the radius of the sphere for the i th species, a surface weight $\delta(R_i-r)$, a mean radius weight $1/8\pi\delta'(R_i-r)$ and finally a weight that does not have the obvious geometrical interpretation of the previous ones $-1/8\pi\delta''(R_i-r)+1/2\pi\delta'(R_i-r)$ and which will not be needed in our derivation for reasons explained later below.

One can easily verify that integrating these weights with respect to \mathbf{r} gives, respectively, the volume, surface and radius of a sphere, and unity for the last one, thus recovering naturally the SPT variables.

Such weights can be generalized to arbitrary convex shapes, introducing the following expressions which derivation is sketched in Appendix A. In what follows $\mathbf{R}(\Omega)$ is the vector to the surface of the convex object measured in the molecular frame, that is the frame oriented by the Euler angle Ω . The volume weight is

$$w_i^{(3)}(\mathbf{r}, \Omega) = \frac{1}{\omega} H(|\mathbf{r}-\mathbf{R}_i(\Omega)|); \quad (16)$$

the surface weight is

$$w_i^{(2)}(\mathbf{r}, \Omega) = \frac{1}{\omega} \sqrt{1 + \frac{1}{r^2} \left(\frac{dR_i(\Omega)}{d\theta} \right)^2} \left[1 + \frac{1}{r^2 \sin^2 \theta} \left(\frac{dR_i(\Omega)}{d\phi} \right)^2 \right] \times \delta(R_i(\Omega) - r); \quad (17)$$

and finally the mean radius weight is

$$w_i^{(1)}(\mathbf{r}, \Omega) = \frac{J(\Omega)\hat{R}_i(\Omega) \cdot \hat{u}}{8\pi\omega} \frac{d}{dr} \delta(R_i(\Omega) - r), \quad (18)$$

where \hat{u} is a unitary vector perpendicular to the surface of the molecular specie i at the point $\mathbf{R}_i(\Omega)$, and ω the solid angle. These weights give the correct definitions for the volume, surface, and mean radius of convex molecules and they reduce directly to the weights of a hard sphere. Again the last weight $w_i^{(0)}$ has been neglected on purpose for reasons that will become clear in the next section.

In order to gain some hint about the geometrical functions involved in the weighted density approximation presented above, it is interesting to examine closely the weight combinations that appear at the pair DCF level from Eq. (3). Using the commutativity of the partial differentiations of the excess free energy Eq. (5) $\Phi_{\alpha\beta} = \Phi_{\beta\alpha}$, we see that the following combinations will appear naturally: The volume of the intersection of the two molecules

$$\Delta V_{ij}(1,2) = w_i^{(3)}(1) \star w_j^{(3)}(2); \quad (19)$$

the surface of the intersection of the two molecules

$$\Delta S_{ij}(1,2) = w_i^{(2)}(1) \star w_j^{(3)}(2) + w_i^{(3)}(1) \star w_j^{(2)}(2); \quad (20)$$

the mean radius of the intersection of the two molecules

$$\Delta R_{ij}(1,2) = w_i^{(1)}(1) \star w_j^{(3)}(2) + w_i^{(3)}(1) \star w_j^{(1)}(2). \quad (21)$$

Other combinations might appear but they do not have the simple meaning of the expressions above. We note in addition that all these quantities are isotropic in the limit $k=0$, as expected. The level of approximation and geometrical meaning will depend on the actual form of the free energy density Φ . If one chooses the scaled particle (SPT) expression for the compressibility PY free energy density Eq. (5), then one gets the following distinct nonzero second derivatives $\Phi_{(3n)}^{\text{PY}_c}$ ($n=0,3$) and the following equalities: $\Phi_{(30)}^{\text{PY}_c} = \Phi_{(21)}^{\text{PY}_c}$, $\Phi_{(31)}^{\text{PY}_c} = \Phi_{(22)}^{\text{PY}_c}/(4\pi)$.

A fourth combination of weights also appears in the pair DCF, and which incorporates the weight $w_i^{(0)}$ that we have neglected

$$w_i^{(0)}(1) \star w_j^{(3)}(2) + w_i^{(3)}(1) \star w_j^{(0)}(2) + w_i^{(1)}(1) \star w_j^{(2)}(2) + w_i^{(2)}(1) \star w_j^{(1)}(2). \quad (22)$$

For the particular case of hard spheres, this combination is exactly identical to the Mayer function¹³ $f_{ij}(1,2)$, but this identity seems to be a feature unique to hard spheres. It is no longer true for disks in two dimensions,²⁶ and for convex bodies as shown here. This is the starting point of our approximations.

1. First approximation for DCF

With the SPT free energy derivatives one can construct a first PY-like DCF from Eq. (3) which indeed will reduce to the exact PY solution in the case of hard spheres mixtures.

$$-C_{ij}(1,2) = \Phi_{(33)}^{\text{PY}_c} \Delta V_{ij}(1,2) + \Phi_{(32)}^{\text{PY}_c} \Delta S_{ij}(1,2) + \Phi_{(31)}^{\text{PY}_c} \left[\Delta R_{ij}(1,2) + \frac{1}{4\pi} w_i^{(2)}(1) \star w_j^{(2)}(2) \right] - \Phi_{(30)}^{\text{PY}_c} f_{ij}(1,2). \quad (23)$$

In this approximation we have simply substituted the Mayer function to the ill-behaved weights combination of Eq. (22). The introduction of the Mayer function here, guaranties the anisotropy at $k=0$ and at contact that is found in the correct PY solution. Moreover, this solution guaranties by construction that the equation of state from the compressibility route is given by the SPT-type equations for $P^* = \beta P$

$$P_c^* = \frac{\xi_0}{1-\xi_3} + \frac{\xi_1 \xi_2}{(1-\xi_3)^2} + \frac{1}{12\pi} \frac{\xi_2^3}{(1-\xi_3)^3}. \quad (24)$$

The corresponding SPT virial equation of state is

$$P_v^* = \frac{\xi_0}{1-\xi_3} + \frac{\xi_1 \xi_2}{(1-\xi_3)^2} + \frac{1}{12\pi} \frac{\xi_2^3}{(1-\xi_3)^2}. \quad (25)$$

However, this last expression will not coincide with the virial EOS which is consistent with our approximation. Both expressions are compared in the results section with the numerical results of the PY approximation. The third term in the r.h.s. of Eq. (23) contains both the mean radius term Eq. (21) and another involving only the surface weight. For hard spheres, this expression gives the mean radius of the convex envelope of the two spheres which is a spherocone.¹² However, for other convex bodies this term is very unlikely to

have the same meaning. Indeed, the numerical results disagree strongly with the PY results. Attempting to correct for this, leads us to the second approximation.

2. Second approximation for DCF

The Percus–Yevick DCF for the hard spheres mixtures can also be cast in the form of the sum involving only the overlap volume and surface terms, as well as the Mayer function. The reason for this can be found in the fact that the third term in Eq. (23) involving the mean radius term, can be rewritten into a surface term plus another involving the Mayer function

$$\begin{aligned} \Delta R_{ij}(1,2) + \frac{w_i^{(2)}(1) \star w_j^{(2)}(2)}{4\pi} \\ = \frac{\Delta S_{ij}(1,2)}{4\pi(R_{mi} + R_{mj})} - f_{ij}(1,2) \frac{R_{mi}R_{mj}}{R_{mi} + R_{mj}}. \end{aligned} \quad (26)$$

This relation holds only for hard spheres mixtures. At $k=0$, this relation involves only the SPT variables, and it can be verified easily that this relation is no longer true for any nonspherical convex body. Using, however, the same relation in the general expression Eq. (23), one gets a second approximation for the pair DCF which depends only on the overlap volume, surface and the Mayer function, and for which the density dependent coefficients can be derived from the SPT free energy. It must be corrected, however, at $k=0$ in order to give the correct SPT compressibility. This gives

$$-C_{ij}(1,2) = \lambda_3 \Delta V_{ij}(1,2) + \lambda_2 \Delta S_{ij}(1,2) - \lambda_0 f_{ij}(1,2)$$

with

$$\lambda_3 = \Phi_{(33)}^{\text{PY}_c}, \quad (27)$$

$$\lambda_2 = \Phi_{(32)}^{\text{PY}_c} + \frac{\Phi_{(31)}^{\text{PY}_c}}{4\pi(R_{mi} + R_{mj})} \gamma, \quad (28)$$

$$\lambda_0 = \Phi_{(30)}^{\text{PY}_c} + \Phi_{(31)}^{\text{PY}_c} \frac{R_{mi}R_{mj}}{R_{mi} + R_{mj}} \gamma,$$

where γ is introduced to give the correct SPT compressibility at $k=0$

$$\gamma = \frac{[(R_{mi}V_j + R_{mj}V_i) + S_i S_j / (4\pi)](R_{mi} + R_{mj})}{(S_i V_j + S_j V_i) / (4\pi) + R_{mi} R_{mj} (V_i + V_j + R_{mi} S_j + R_{mj} S_i)}.$$

The approximation is justified through the good agreement obtained with the PY numerical results for the pair DCF, and by the fact that the term replaced was not meaningful for general convex bodies. In addition, the EOS obtained through the compressibility route is still given by the SPT expression Eq. (5). This second approximation is not as ad hoc as it may seem, because for hard spheres, the PY pair DCF can be written only in terms of the overlap volume, overlap surface and the Mayer function, and this can be extended to convex objects, as shown below for the third approximation.

3. Third approximation for DCF

This approximation is derived here for a single component system and its generalization to mixtures rests on an ansatz. The form of the pair DCF is similar to the previous approximation, but the density dependent factors are computed in a self-consistent manner. We note that for hard spheres the pair DCF can be written as

$$C^{\text{PY-HS}}(r) = \alpha_3 \Delta V(r) + \alpha_2 \Delta S(r) + \alpha_0 f(r), \quad (29)$$

where $\Delta V(r)$ is the overlap volume between the hard spheres separated by distance r , $\Delta S(r)$ is the corresponding surface, and the coefficients can be derived unambiguously through the sole knowledge of the virial and compressibility EOS. These coefficients are given by $\alpha_3 V = -\eta(1+2\eta)^2/(1-\eta)^4$, $\alpha_2 S = -4.5\eta(1+\eta)/(1-\eta)^3$, $\alpha_0 = 0.5(2+\eta)/(1-\eta)^2$, where $\eta = (\pi/6)\rho\sigma^3$ is the packing fraction, V is the HS volume and S the surface. This particular form is generalizable to angle dependent hard core molecules in a straightforward manner. We demonstrate below how this expression can be obtained directly from the knowledge of the compressibility and virial equations of state (EOS), for which one could select in particular the SPT form given by Eqs. (24) and (25). A similar form without the surface term has been proposed by Rickayzen and co-workers.¹¹ Their method involves a DCF defined for restricted orientations with the consequence of being fully analytical, particularly for the Mayer function. The method outlined below includes the surface term and is free of the restriction over orientations.

We write

$$C(1,2) = \alpha_3 \Delta V(1,2) + \alpha_2 \Delta S(1,2) + \alpha_0 f(1,2). \quad (30)$$

Then the three coefficients can be calculated in the following way. α_0 can be calculated from the value of $C(1,2)$ at contact, and the virial EOS Z_v . In the case of the PY-type solution we have the following relation between the pair distribution function and the DCF at contact $\sigma(1,2)$: $g(\sigma(1,2)) = -C(\sigma(1,2))$. From the expression for the virial EOS²⁷ we get

$$\alpha_0 = \frac{Z_v - 1}{\rho B_2}, \quad (31)$$

where B_2 is the second virial coefficient.

The remaining two coefficients can be evaluated from two coupled equations. The compressibility equation $1 - \rho \tilde{C}^{000}(k=0) = \partial \beta P / \partial \rho = \chi_0 / \chi_T$ gives

$$\alpha_3 V + 2\alpha_2 S = \frac{2Z_c - 1 - (\chi_0 / \chi_T)}{\xi_3}, \quad (32)$$

where we have used the definition of α_0 , and the fact that $\Delta \tilde{V}^{000} = V^2$ and $\Delta \tilde{S}^{000} = 2VS$, where V is the volume of the convex molecule and S its surface. At zero separation $r=0$ we also have, from the Ornstein–Zernike equation

$$C(r=0,12) = -\frac{\chi_0}{\chi_T} - \frac{\rho}{\omega^2} \int d\mathbf{r} d\Omega_3 g(\mathbf{r},13) C(\mathbf{r},32). \quad (33)$$

In the particular case of the PY approximation, the product inside the integral is exactly zero for identical orientations $\Omega_1 = \Omega_2$. In our case this will not be true, as the pair correlation function derived from our approximate DCF will not be zero inside the hard core in general, however, we assume this as an additional approximation. Then by noting that for these particular orientations we have $\Delta_V(r=0, \Omega, \Omega) = V$ and $\Delta_S(r=0, \Omega, \Omega) = S$ we obtain the second equation

$$\alpha_3 V + \alpha_2 S = \alpha_0 - \chi_0 / \chi_T. \quad (34)$$

The two equations (32) and (34) can be solved trivially with the SPT equation of state Eq. (5). One can readily check that the solution thus obtained reduces to the hard sphere PY solution for the DCF. This approximation can be extended to mixtures by using the following ansatz. One can keep the same density dependent coefficients, and account for different species through the weights factors. This is in the spirit of the WDFT expression for DCF. Unfortunately, this ansatz will not give the correct expressions for DCF of the hard spheres mixtures. The reason is that this last approximation does not derive from the SPT functional.

C. Common features

All three approximations yield the SPT equation of state through the compressibility equation. They have different virial EOS as they lead to independent pair distribution functions.

They are independent of the order of expansion in the invariants. This can be seen from Eq. (14). This feature makes the approximations quite appealing, as one could compute separately any projections $C_{\mu\nu}^{mnl}$ which might be of particular interest, such as \tilde{C}_{00}^{000} which is related to the compressibility,¹ or \tilde{C}_{00}^{220} which is related to the Kerr constant and the orientational instability of the isotropic phase. This property makes these approximations particularly suited to study biaxial convex bodies. In contrast, for such cases, conventional methods like integral equation approaches, will involve larger sets of invariants, because of the third Euler angle, and will become rapidly numerically cumbersome. All three approximations are PY-like, in the sense that the pair DCF is zero outside the hard core.

None of these approximations will guaranty that the corresponding pair correlation function is rigorously zero inside the hard core. However, this point can be regarded as being relatively minor if one wants to focus solely on the pair DCF within density functional type approaches. To take into account this stringent constraint on the pair distribution function is not easy, and certainly the semi-analytic nature of the present approximations must be abandoned if one would try to incorporate this constraint. However, the expansion coefficients of the pair correlation function, as obtained by inverting the OZ equation are in good agreement with PY results, but only at small elongations, and in the low to medium density range. This is expected from the good agreement obtained for the C^{mnl} in the same conditions, as discussed in the next section.

III. RESULTS

The numerical applications are restricted to single component fluids which have been studied more often in the past literature.²⁸ Only convex particles are studied here, mainly because the formalism is by construction better suited for these objects. In view of the applications of the SPT theory,¹⁸ it is expected to give good results for fused hard spheres of moderate aspect ratios. Applications of the present approximations to such models will be presented in another context.

A. Equation of state

Before comparing the approximations of the pair DCF to those obtained for PY theory, it is interesting to analyze the accuracy of the SPT EOS, both virial and compressibility route when compared to those obtained by solving numerically the PY theory. This is a zero-moment test of the DCF. Figures 1(a)–1(c) show the reduce pressure $\beta P V_m$ vs $\eta = \rho V_m$ (V_m is the molecular volume) for different theories and different convex objects. Results obtained from the SPT theory Eq. (24) and Eq. (25) are plotted in lines. Those obtained by solving numerically the PY theory are shown in open circles for the compressibility route and in filled circles for the virial route. Results for ellipsoids²⁷ are in Fig. 1(a), for prolate²⁹ and oblate³⁰ spherocylinders in Fig. 1(b) and for cut spheres³¹ in Fig. 1(c). It is clear that the SPT theory is only an approximation to the true PY results, even though the agreement is near perfect at small elongations. This is another proof for the fact that the WDFT is unable to reproduce the correct PY DCF.

We have noted empirically that an accurate EOS for convex objects can be obtained by using a Carnahan and Starling (CS) type combination $Z = (2Z_c + Z_v)/3$. These results are also plotted in full lines in all the figures, together with those available through computer simulations for ellipsoids,³² for spherocylinders,³³ and for cutspheres.³⁴ The agreement is quite remarkable, especially for aspect ratios smaller than 3 and for the full density range of the isotropic phase. The prolate–oblate symmetry observed in the simulations for ellipsoids is also well reproduced. However, the accuracy decreases for aspect ratios very different from unity, especially for cutspheres in Fig. 1(c), and the curvature of the EOS at high density tends to increase more upwards for the theory. This can be explained from the numerical results for higher order virial coefficients² which become negative in the large aspect ratio limit.

In view of the good agreement between the CS equation of state and the simulation results, one can calculate analytically virial coefficients by taking the limit $\rho \rightarrow 0$. The second virial coefficient known exactly for convex bodies¹⁷ is $B_2 = V + R_m S$, which is recovered exactly by the PY and the SPT equation of state. The third virial coefficient is also exact from PY theory,¹ but the SPT equations of state does not give the correct values for convex bodies other than hard spheres. The SPT-CS expressions for virial coefficients obtained in terms of the SPT geometrical variables, are given by a single formula

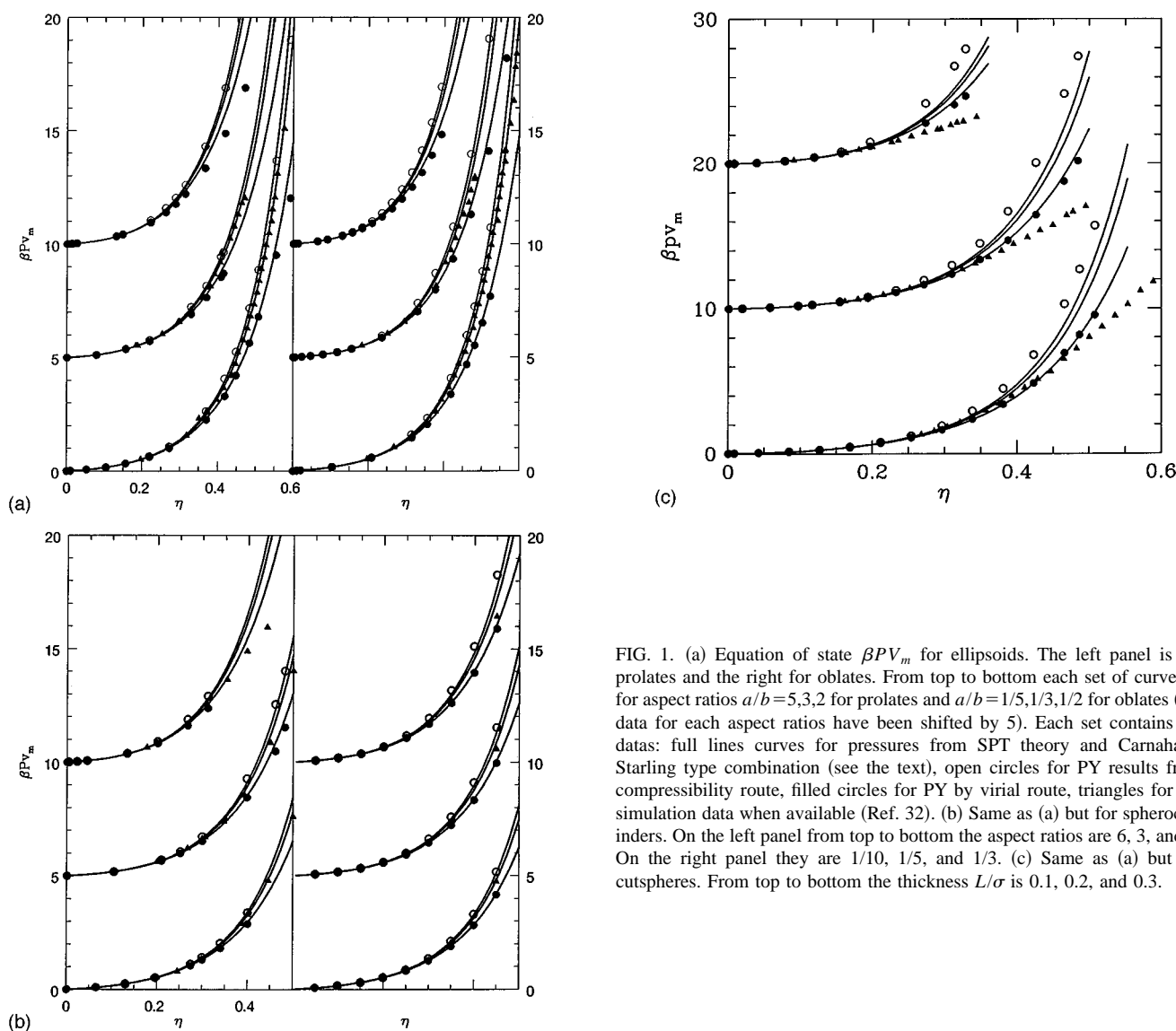


FIG. 1. (a) Equation of state $\beta P V_m$ for ellipsoids. The left panel is for prolates and the right for oblates. From top to bottom each set of curves is for aspect ratios $a/b=5,3,2$ for prolates and $a/b=1/5,1/3,1/2$ for oblates (the data for each aspect ratios have been shifted by 5). Each set contains six data: full lines curves for pressures from SPT theory and Carnahan–Starling type combination (see the text), open circles for PY results from compressibility route, filled circles for PY by virial route, triangles for the simulation data when available (Ref. 32). (b) Same as (a) but for spherocylinders. On the left panel from top to bottom the aspect ratios are 6, 3, and 2. On the right panel they are 1/10, 1/5, and 1/3. (c) Same as (a) but for cutspheres. From top to bottom the thickness L/σ is 0.1, 0.2, and 0.3.

$$B_n = V^{n-1} + (n-1)R_m S V^{n-2} + \frac{n(n-2)}{36\pi} S^3 V^{n-3}. \quad (35)$$

Virial coefficients of different orders and for different convex bodies are shown in Figs. 2(a)–2(c), and compared with several simulation results. In view of the simplicity of the SPT expressions, the agreement can be considered relatively good, mainly at moderate aspect ratios. One can note that some of the exact B_5 tend to become negative, which is never the case for those from expression above, and at any order.

B. Pair direct correlation function

The pair DCF for single component convex body fluids is obtained through the calculations of the volume, surface, and mean radius terms Eqs. (19)–(21). These are in turn computed through the weights evaluated in the fourier space. Analytical expressions for the expansion coefficients of the

weights of some convex bodies are listed in Appendix B. The Mayer function expansion coefficients must be computed numerically. One can note that these coefficients are related to the overlap coefficients used in the numerical solution for the PY and HNC theory²⁷ by the relation $f^{mnl}(r) = -A_{000}^{mnl}(r)$, and which numerical computation has been detailed elsewhere.²⁷

In Fig. 3 all three approximations are compared for an ellipsoid of aspect ratio 3, in the following way: the density dependent factors in Eqs. (23), (27), (30) are plotted, in full lines for model 1, dotted lines for model 2 and dashed lines for model 3. There is very little dispersion for volume and surface coefficients between the three theories. The coefficient in front of the Mayer coefficient is much smaller for the first model, the mean radius term providing some numerical compensation in this case.

In Fig. 4 six of the expansion coefficients for the different pair DCF are plotted for the hard ellipsoids fluid of as-

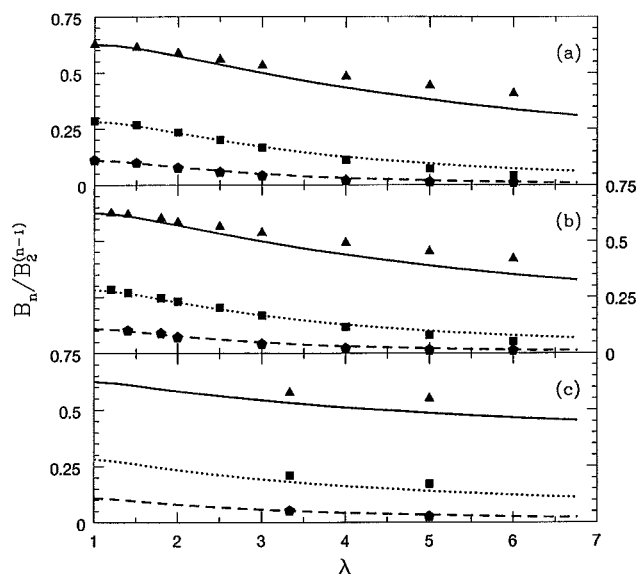


FIG. 2. Virial coefficients B_n/B_2^{n-1} for $n=3,4,5$ plotted versus the aspect ratio. Calculated results for B_3^* as obtained from the expansion of CS type EOS (see the text) are shown in full lines, dotted lines for B_4^* and dashed lines for B_5^* . Top panel is for ellipsoids, middle one for spherocylinders and bottom one for cutspheres. Simulation data for B_n^* are represented by n -sided polygon, for ellipsoids (Ref. 35), for spherocylinders (Ref. 28), and for cutspheres (Ref. 34).

pect ratio 3, at the reduced density $\rho^* = \rho\sigma^3 = 0.25$, where σ is the smallest diameter of the ellipsoid. The first approximation for the pair DCF (in dashed lines) is clearly the worst approximation. As noted in Sec. II B 1, the third term in this approximation Eq. (23) is the incorrect mean radius term for the convex envelope of the intersection of two convex bodies. The large deviations near $r=0$ are due precisely to the double surface convolution term appearing in Eq. (23). A

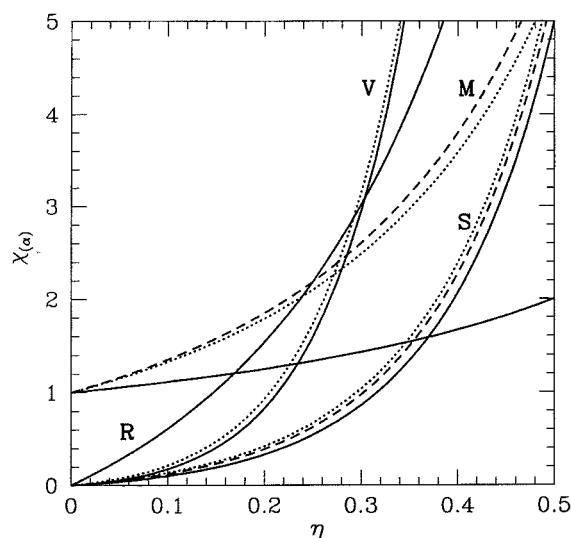


FIG. 3. Density dependent coefficients for the pair DCF for ellipsoid of aspect ratio 3, and for the three models presented in this work. Full, dotted and dashed lines are, respectively, for first, second, and third approximations. The letters help identifying coefficients of volume (V), surface (S), Radius (R) and the Mayer function (M) terms.

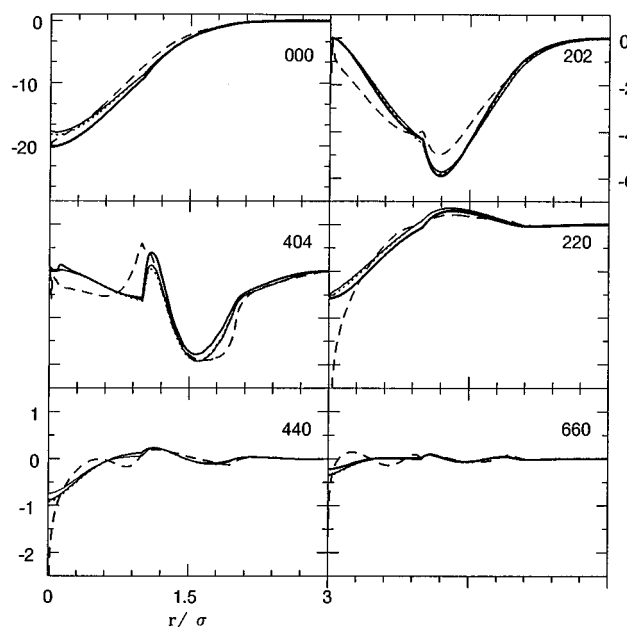


FIG. 4. Selected harmonics from the direct correlation function for ellipsoids of aspect ratio 3 for density $\rho^*=0.25$. Thicker full line for numerical solution of PY theory, full line for the second approximation, dotted line for the third, and dashed line for the first.

correct version of this term might give better results, but it is not obvious that it will be written as a convolution. The second and third approximations are closer to the PY results and the agreement is very good, especially in view of the high liquid density (the instability of the isotropic phase occurs⁶ near $\rho^*=0.29$, and the PY theory could be solved only up to $\rho^*=0.28$). In Fig. 5(a) the pair DCF is plotted for an ellipsoid of aspect ratio 5 at density $\rho^*=0.12$ which also represent a high density. Only the last two approximations are plotted together with the PY results. Again, we note that they give results that are quite close to each other. The agreement is slightly worse near $r=0$, but this is a high density behavior, the agreement being surprisingly good at lower densities, and over the whole density range for smaller aspect ratios.

Similar comparisons are made in Fig. 5(b) for oblate ellipsoid of aspect ratio 1/3, at density $\rho^*=0.11$; in Fig. 5(c) for spherocylinder of aspect ratio 6 at density $\rho^*=0.1$; in Fig. 5(d) for cut spheres of reduced thickness $L/\sigma=0.2$ at density $\rho^*=0.022$.

The general features are very similar to that obtained in Fig. 5(a). One can note that the agreement tend to deteriorate for oblate shapes in general, especially at small thickness. The densities given here have been taken at densities close to the highest at which the PY could be solved numerically. In all cases the agreement is quite good at moderate densities.

The proximity of the last two approximations is simply due to the similarity between the numerical values of the density dependent prefactors as seen in Fig. 3.

In view of the simplicity and generality of the second approximation, as opposed to the last approximation, it is clear that it is the best candidate for a PY-like approximation.

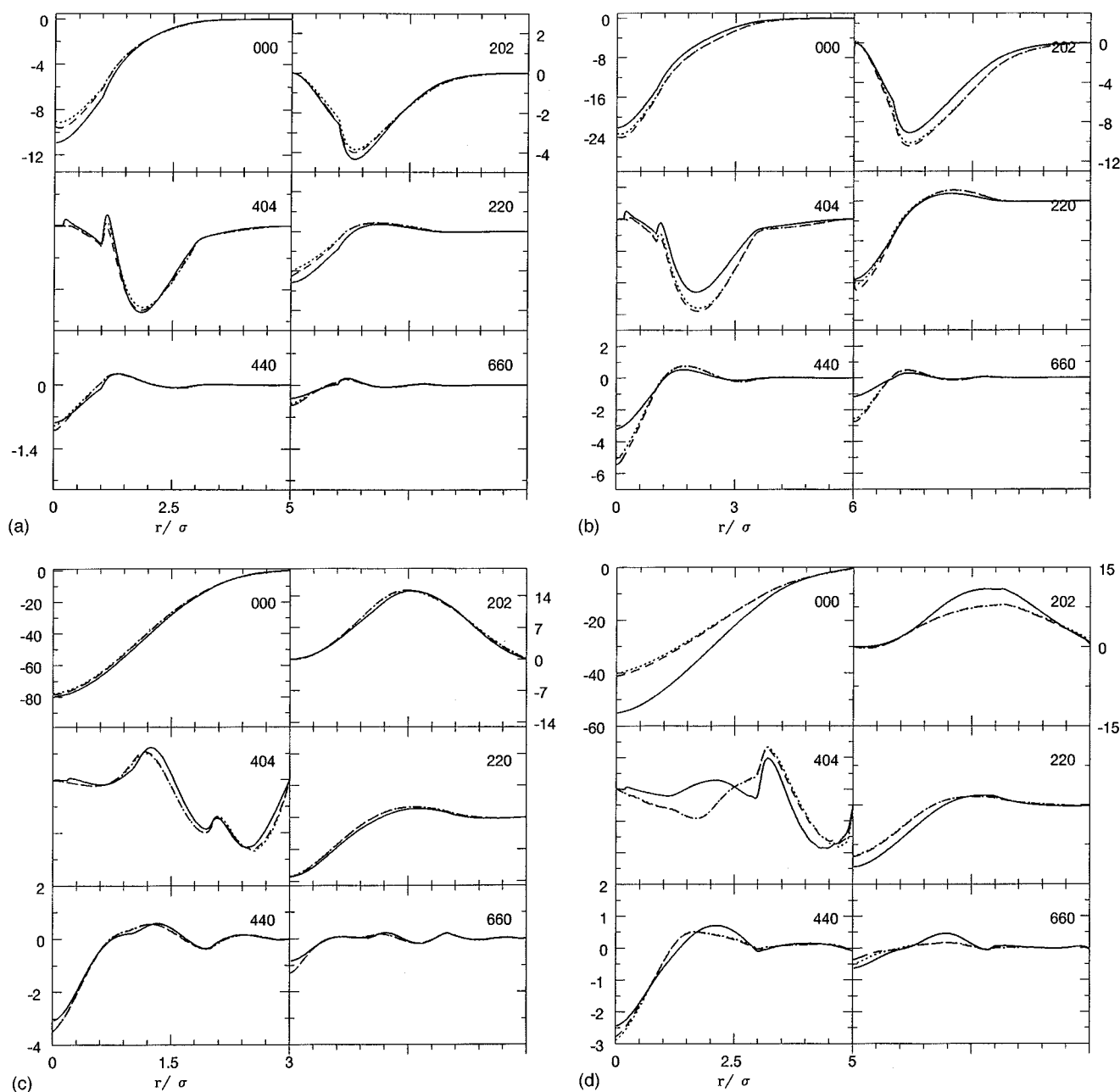


FIG. 5. (a) Selected harmonics from the direct correlation function for prolate ellipsoids of aspect ratio 5 for density $\rho^*=0.12$. Full line for the PY results and dotted line for the second approximation. (b) Same as (a) but for oblate ellipsoids of aspect ratio 1/3 for density $\rho^*=0.11$. (c) Same as (a) but for prolate spherocylinders of aspect ratio 5 for density $\rho^*=0.1$. (d) Same as (a) but for cutspheres of thickness 0.2 for density $\rho^*=0.022$.

C. The instability of the isotropic phase

In previous work^{6,27,29} it was found that the PY theory could not predict the instability of the isotropic phase, as opposed to the HNC theory. This instability was measured through the expression for the Kerr constant $K^* = \Delta_2 = 1 - \rho \tilde{C}^{220}(k=0)$ which was found to decrease to zero faster for HNC theory. For the latter solutions could not be obtained for densities such that K^* approaches zero, mainly due to the numerical difficulties coming from the long ranged behavior of the pair correlation component

$h^{220}(r)$. The origin of loss of solutions for the PY theory is less clear, as no such long range features were observed in this function.

The present approximations, despite their analogy with PY theory, are free from this anomaly. This is depicted in Figs. 6(a)–6(c) for some convex bodies, through the plot of Δ_2 . In contrast with HNC or PY theories, numerical values for the pair DCF can be obtained even for densities such that $\Delta_2 \leq 0$. Only the last two approximations are plotted, together with the PY and HNC results when available. A noticeable

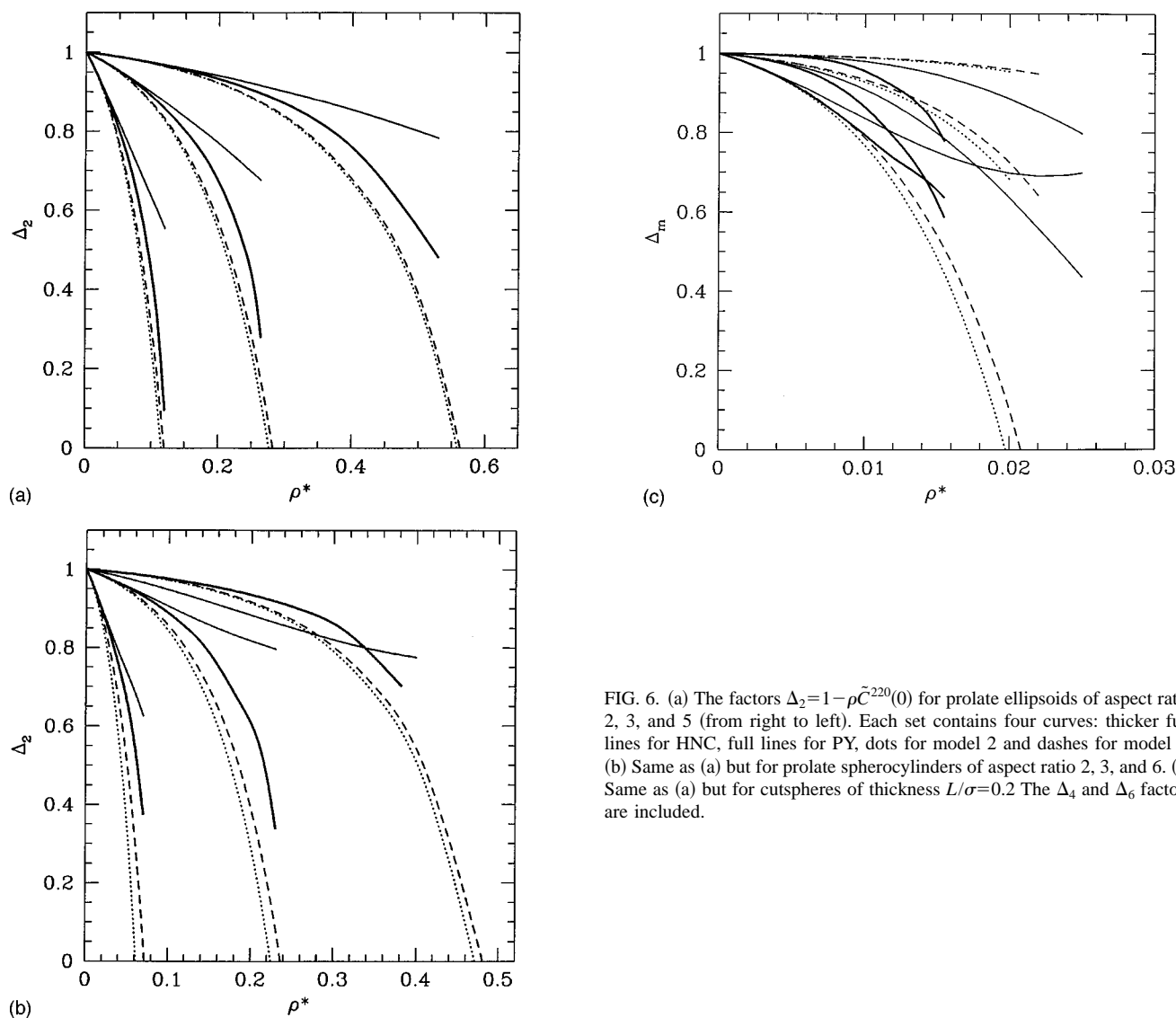


FIG. 6. (a) The factors $\Delta_2 = 1 - \rho \tilde{C}^{220}(0)$ for prolate ellipsoids of aspect ratio 2, 3, and 5 (from right to left). Each set contains four curves: thicker full lines for HNC, full lines for PY, dots for model 2 and dashes for model 3. (b) Same as (a) but for prolate spherocylinders of aspect ratio 2, 3, and 6. (c) Same as (a) but for cutspheres of thickness $L/\sigma=0.2$. The Δ_4 and Δ_6 factors are included.

feature is that the Δ_2 values for both approximations are very much HNC like. In particular, the instability density is close to that of HNC. This happens even though the pair DCF coefficient $C^{220}(r)$ is quite different from those obtained by solving HNC (the instability of HNC is obtained through the growth of a small positive tail outside the hard core). But the higher order terms Δ_m for $m=4$ and $m=6$ have a PY-like behavior and do not contribute to destabilize the isotropic phase. It was observed that for HNC this destabilization occurs through all the modes Δ_m .^{6,27}

For the cut spheres, it was shown by computer simulations³⁴ that the destabilization of the isotropic phase can occur through the term Δ_4 for thickness of $L/\sigma=0.2$, and a transition to *cubic* phase was observed. In Fig. 6(c) we have plotted the results for all Δ_m for HNC³¹ (in thicker full line), PY³¹ (full lines) and the last two approximations for DCF (dotted and dashed curves, respectively). It is clear that both HNC and PY theory show a tendency to cubic order, with a clear tendency to destabilization shown only for the HNC results. In contrast, the approximations for the DCF

indicate a destabilization through Δ_2 . The reason for this can be found in the fact that both approximations are linear in the Mayer function in the limit $k=0$, as can be seen from Eqs. (27) and (30), which give the only nonzero contribution in the same limit. In that sense they will behave like Onsager-type models for which the destabilization through Δ_4 is absent.³¹

IV. CONCLUSION

The main conclusion of this work is that it is possible to construct PY-like approximations for the pair DCF based on a geometrical approach, and which are in good quantitative agreement with the true PY pair DCF. Such approximations are expressed solely in terms of the overlap volume, the overlap surface, and the Mayer function, with prefactors dependent on the density and elementary geometrical features of the hard core models (volume, surface, and mean radius) through the SPT variables. All approximations are semianalytical, and independent of the order of expansion in rota-

tional invariants, which make them suitable to study complex molecular geometries such as biaxial ellipsoids for instance.

It is shown that the PY solution cannot be obtained through convolutions of weight functions, due mainly to the inherent isotropy at $k=0$ contained within such approach. The overall agreement obtained with the second approximation makes it a good candidate for further studies. In particular, there are very little results for mixtures of convex bodies in the literature.³⁷ This is also the case for biaxial hard cores, for which some conjectures on the type of smectic phases have been proposed.⁵ However, the Onsager like character of these approximations, in the limit $k=0$, may be an obstacle for this purpose, unless further corrections are included.

The fact that these approximations are based on a free energy functional make them easy to be extended to inhomogeneous systems. In view of the success of such theories for hard spheres interfacial properties^{13,14,36} one can expect similar results for anisotropic liquid–solid interfaces. More importantly, these methods can be used to study orientationally inhomogeneous liquids such as unorientated nematics for which little is known from integral equation theories.³⁸ Such applications are currently under investigation.

ACKNOWLEDGMENTS

The authors wish to thank Y. Rosenfeld, M. Moreau, and M. L. Rosinberg for many discussions and comments.

APPENDIX A: WEIGHT FUNCTIONS

In what follows the molecular specie index i will be abandoned since the weights depend only on the single specie geometrical parameters. The weight functions are constructed under the two constraints. First, they should yield at $k=0$ the SPT variables $R^{(\alpha)}$ of the hard convex molecule, which are the volume $R^{(3)}=V$, the surface $R^{(2)}=S$ and the mean radius $R^{(1)}=R_m$. This is expressed as

$$R^{(\alpha)} = w^{(\alpha)}(k=0). \quad (\text{A1})$$

In addition, the weights must reduce to their corresponding expressions in the hard sphere limit.¹⁴ These conditions will not in general determine uniquely the weight functions. The expressions given here are straightforward extension of the hard spheres weights.¹⁴ The volume weight is most easily constructed using the Heaviside function $H(|\mathbf{r}-\mathbf{R}(\Omega)|)/\omega$, where $\mathbf{R}(\Omega)$ is a vector connecting the center of mass of the molecule (oriented by the Euler angle Ω) to its surface, and ω is the solid angle appropriate to the geometry of the molecule. The notation $\mathbf{R}(\Omega)$ indicates that vector \mathbf{R} is measured in the molecular frame, which is oriented by the Euler angle Ω . It can be checked in a straightforward manner that this weight yields the correct volume. In particular, the intersection volume of two objects is nicely given by Eq. (19).

The surface weight can be computed from an integral over the elementary surface element. In the molecular frame, for vector $\mathbf{R}=(R,\theta,\phi)$ one obtains the following expression for the elementary surface element ds :

$$\begin{aligned} ds &= R^2 \sin \theta \\ &\times \sqrt{\left[1 + \frac{1}{r^2} \left(\frac{dR(\Omega)}{d\theta}\right)^2\right] \left[1 + \frac{1}{r^2 \sin^2 \theta} \left(\frac{dR(\Omega)}{d\phi}\right)^2\right]} \\ &\times dR \, d\theta \, d\phi. \end{aligned} \quad (\text{A2})$$

The total surface is then simply given by

$$S = \int ds \, \delta(R-r). \quad (\text{A3})$$

Noting that in the general frame, the orientation of vector \mathbf{R} can be measured with respect to the molecular axis orientation Ω the expression in Eq. (17) is immediately recovered. In the spherical case, R is independent of the orientation and Eq. (17) gives $\delta(R-r)$ which is the spherical surface weight.¹⁴

The mean radius weight is computed by an integral condition similar to the surface weight. The definition of the mean radius is^{17,39}

$$R_m = \frac{1}{4\pi} \int d\hat{u} \, \mathbf{R} \cdot \hat{u}, \quad (\text{A4})$$

where \hat{u} is a unitary vector orthogonal to the surface of the molecule at the point given by \mathbf{R} . From this integral relation and Eq. (A1) one can derive the mean radius weight with a form similar to that for hard spheres.¹⁴ First one must transform the integral over \hat{u} into an integral over the angular variables (θ, ϕ) corresponding to the orientation of \mathbf{R} in the intermolecular frame. Defining by $J(\theta, \phi)$ the jacobian of the transformation one obtains directly Eq. (18).

The volume weight is expanded in a straightforward manner through the general relation

$$w^{(\alpha)m\mu}(r) = \frac{1}{I_m} \int w^{(\alpha)}(\mathbf{r}, \Omega) \overline{\Phi_{\mu 0}^{m0m}}(\Omega, \hat{r}) d\hat{r} \, d\Omega, \quad (\text{A5})$$

where

$$\begin{aligned} I_m &= \int \Phi_{\mu 0}^{m0m}(\Omega, \hat{r}) \overline{\Phi_{\mu 0}^{m0m}}(\Omega, \hat{r}) d\hat{r} \, d\Omega, \\ &= 4\pi \omega \left(\frac{f^{m0m}}{2m+1} \right)^2. \end{aligned}$$

However, the surface and mean radius weights are distributions and some care must be taken when applying above relation. The generic term of these two weights, as defined by Eqs. (17) and (18), can be written in the molecular frame as

$$w^{(\alpha)}(r, \theta, \phi) = F(\theta, \phi) \delta^{(n)}(r - R(\theta, \phi)), \quad (\text{A6})$$

where the subscript (n) indicate the order of the derivative of the Dirac δ function with respect to r , with $n=0$ for surface weight and $n=1$ for the mean radius term, and the function $F(\theta, \phi)$ can be deduced from inspection of Eq. (17) and Eq. (18). Changing from the variables (θ, ϕ) to (R, ϕ) we get

$$w^{(\alpha)m\mu}(r) = \frac{1}{\omega} \int_0^{2\pi} d\phi \int dR \frac{\sin[\theta(R, \phi)] F(R, \phi)}{(dR/d\theta)(R, \phi)} \times \delta^{(n)}(r-R), \quad (\text{A7})$$

where the denominator is the Jacobian of the transformation and is understood to be a function of R and ϕ . The inner integral is trivially integrated when $n=0$ and must be integrated by parts for $n=1$.

For axially symmetric molecules, the expressions tend to simplify greatly. The rotational invariant in Eq. (7) can be expressed as a Legendre polynomial in term of the single angle θ between the molecular axis and the vector \mathbf{R} , by using the addition theorem of the spherical harmonics

$$\Phi^{m0m}(\hat{r}, \Omega) = \frac{f^{m0m}(-)^m}{\sqrt{2m+1}} P_m(\hat{r} \cdot \Omega), \quad (\text{A8})$$

where the dot indicates a dot product. By choosing the convention $f^{m0m} = \sqrt{2m+1}$ which is the Blum convention^{20,27} one gets the following simplified expressions for the expansion coefficients of all the weights:

volume weight

$$w^{(3)m}(r) = \frac{(2m+1)^{3/2}}{\omega f^{m0m}} \int_{r < R(\theta)} d\theta \sin \theta P_m(\cos \theta); \quad (\text{A9})$$

surface weight

$$w^{(2)m}(r) = \frac{(2m+1)^{3/2}}{\omega f^{m0m}} \frac{\sin \theta}{(dr/d\theta)} \sqrt{1 + \frac{1}{r^2} \left(\frac{dr}{d\theta} \right)^2} P_m(\cos \theta), \quad (\text{A10})$$

where $\theta = \theta(r)$ is the angle corresponding to the radial distance r on the convex body (for $0 \leq \theta \leq \pi/2$).

Mean radius weight

$$w^{(1)m}(r) = \frac{(2m+1)^{3/2}}{\omega f^{m0m}} \frac{d}{dr} \gamma(r) \quad (\text{A11})$$

with

$$\gamma(r) = \frac{\sin \theta P_m(\cos \theta)}{(dr/d\theta)} \frac{J(\theta) \hat{r} \cdot \hat{u}}{8\pi}, \quad (\text{A12})$$

where the last term is related to the mean radius term in Eq. (A4). Again it is understood that θ is a function of r .

The relationship between θ and r can be easily derived for most convex bodies such as those studied in this article. The explicit expressions of the weights are given in Appendix B. The convolution products are evaluated through the numerical Hankel transforms of the weights expansion coefficients.

APPENDIX B: WEIGHT FUNCTIONS FOR SOME CONVEX BODIES

The expansion coefficients for weights are given below for convex bodies with axial symmetry. The index μ in Eq.

(6) associated with the azimuthal angle is then zero and will be systematically omitted here. The following definition $\alpha_m = (2m+1)^{3/2}/f^{m0m}$ is conveniently used in all expressions below.

Weights for ellipsoids

In what follows a and b are, respectively, the largest and smallest principal radii of the ellipsoid.

The volume weight is for $m=0$

$$w^{(3)0}(r) = 1 - \phi(r) \quad \text{and} \quad \epsilon = +1 \quad \text{for prolate,}$$

$$w^{(3)0}(r) = \phi(r) \quad \text{and} \quad \epsilon = -1 \quad \text{for oblate,}$$

and for $m \neq 0$

$$w^{(3)m}(r) = \epsilon \alpha_m \int_{\phi(r)}^1 du P_m(u), \quad (\text{B1})$$

where we have defined the function $\phi(r)$

$$\phi(r) = a/r \sqrt{(b^2 - r^2)/(b^2 - a^2)}. \quad (\text{B2})$$

The surface weight is

$$w^{(2)m}(r) = \alpha_m \xi(r) P_m(\phi(r)) \lambda(r) \quad (\text{B3})$$

with

$$\xi(r) = b/r \sqrt{(a^2 - r^2)/(a^2 - b^2)}$$

and

$$\lambda(r) = ab^2 / (r^2 \sqrt{(a^2 - b^2)(r^2 - b^2)}).$$

The mean-radius weight is

$$w^{(1)m}(r) = \alpha_m P_m(\phi(r)) \lambda(r) \zeta(r) \quad (\text{B4})$$

with

$$\zeta(r) = \frac{a^5 b^3 \sqrt{a^2 - (a^2 - b^2) \phi^2(r)}}{8\pi r (a^4 - (a^4 - b^4) \phi^2(r))^2}. \quad (\text{B5})$$

Prolate spherocylinders

In what follows, σ is the diameter of the spherical cap, and L is the length of the cylinder. We define $\gamma = (L^2 - \sigma^2)/4$ and $R_L = \sigma/2 \sqrt{1 + (L/\sigma)^2}$.

The volume weight is

$$w^{(3)m}(r) = \alpha_m \int_{\phi(r)}^1 du P_m(u), \quad (\text{B6})$$

where the function $\phi(r)$ is defined by

$$\phi(r) = \sqrt{1 - (\sigma/2r)^2} \quad \text{for} \quad \sigma/2 < r < R_L,$$

$$\phi(r) = (r^2 + \gamma)/rL \quad \text{for} \quad R_L < r < (\sigma + L)/2.$$

The surface weight is

$$w^{(2)m}(r) = \alpha_m \kappa(r) P_m(\phi(r)), \quad (\text{B7})$$

where the function $\phi(r)$ is the same as above and $\kappa(r)$ is defined by

$$\kappa(r) = \sigma / (2r^2 \phi(r)) \quad \text{for} \quad \sigma/2 < r < R_L,$$

$$\kappa(r) = \sigma / (rL) \quad \text{for} \quad R_L < r < (\sigma + L)/2.$$

Cut spheres

σ is the sphere diameter, and L is cutsphere thickness. We define for $L/2 < r < \sigma/2$ the following weights: The volume weight is

$$w^{(3)m}(r) = \alpha_m \int_0^{L/2r} P_m(u) du; \quad (\text{B8})$$

the surface weight is

$$w^{(2)m}(r) = \alpha_m P_m(L/2r)/r + \delta(r - \sigma/2) \int_0^{L/\sigma} P_m(u) du. \quad (\text{B9})$$

- ¹J. P. Hansen and I. R. McDonald, *Theory of Simple Liquids* (Academic, London, 1986).
- ²M. P. Allen, G. T. Evans, D. Frenkel, and B. M. Mulder, *Adv. Chem. Phys.* **LXXXVI**, 1 (1993).
- ³R. Evans, in *Inhomogeneous Fluids*, edited by D. Henderson (Dekker, New York, 1992).
- ⁴J. L. Colot, X. G. Wu, H. Xu, and M. Baus, *Phys. Rev. A* **38**, 2022 (1988).
- ⁵A. M. Somoza and P. Tarazona, *J. Chem. Phys.* **91**, 517 (1989).
- ⁶A. Perera, J. J. Weis, and G. N. Patey, *J. Chem. Phys.* **89**, 6941 (1988).
- ⁷R. Pynn, *Solid. St. Commun.* **14**, 29 (1974); *J. Chem. Phys.* **60**, 4579 (1974).
- ⁸H. Xu, H. N. Lekkerkerker, and M. Baus, *Europhys. Lett.* **62**, 800 (1989).
- ⁹H. Xu, *Mol. Phys.* **77**, 311 (1992).
- ¹⁰F. Lado, *Mol. Phys.* **54**, 407 (1985).
- ¹¹G. Rickayzen, *Mol. Phys.* **75**, 333 (1992); M. Calleja and G. Rickayzen, *ibid.* **76**, 693 (1992); P. Kalpaxis and G. Rickayzen, *ibid.* **80**, 391 (1993).
- ¹²Y. Rosenfeld, *J. Chem. Phys.* **89**, 4271 (1988).
- ¹³Y. Rosenfeld, *Phys. Rev. Lett.* **63**, 980 (1989).
- ¹⁴E. Kierlik and M. L. Rosinberg, *Phys. Rev. A* **42**, 3382 (1990).
- ¹⁵Y. Rosenfeld, *Phys. Rev. E* **50**, 3318 (1994).
- ¹⁶J. L. Lebowitz and J. S. Rowlinson, *J. Chem. Phys.* **41**, 133 (1964).
- ¹⁷A. Isihara and T. Hayashida, *J. Chem. Phys.* **6**, 40 (1950); A. Isihara, *ibid.* **19**, 1142 (1956).
- ¹⁸R. M. Gibbons, *Mol. Phys.* **17**, 81 (1969); **18**, 809 (1970).
- ¹⁹S. Phan, E. Kierlik, M. L. Rosinberg, B. Bildstein, and G. Kahl, *Phys. Rev. E* **48**, 618 (1993).
- ²⁰L. Blum and A. J. Torruella, *J. Chem. Phys.* **56**, 303 (1972).
- ²¹M. Abramowitz and I. A. Stegun, *Handbook of Mathematical Functions* (Dover, New York, 1972).
- ²²A. Messiah, *Quantum Mechanics* (Wiley, New York, 1961), Vol. II.
- ²³P. H. Fries and G. N. Patey, *J. Chem. Phys.* **82**, 429 (1985).
- ²⁴C. G. Gray and K. E. Gubbins, *Theory of Molecular Fluids* (Clarendon, Oxford, 1984).
- ²⁵L. Onsager, *Ann. N.Y. Acad. Sci.* **51**, 627 (1949).
- ²⁶Y. Rosenfeld, *Phys. Rev. A* **42**, 5978 (1990).
- ²⁷A. Perera, P. G. Kusalik, and G. N. Patey, *J. Chem. Phys.* **87**, 1295 (1987).
- ²⁸T. Boublík and I. Nezbeda, *Collect. Czech. Chem. Commun.* **51**, 2301 (1986).
- ²⁹A. Perera and G. N. Patey, *J. Chem. Phys.* **89**, 5861 (1988).
- ³⁰J. Šedlbauer, S. Labík, and Malijevský, *Phys. Rev. E* **49**, 3179 (1993).
- ³¹A. Chamoux and A. Perera (unpublished).
- ³²D. Frenkel and B. M. Mulder, *Mol. Phys.* **55**, 1171 (1985); B. M. Mulder and D. Frenkel, *ibid.* **55**, 1193 (1985).
- ³³J. A. C. Veerman and D. Frenkel, *Phys. Rev. A* **41**, 3237 (1990).
- ³⁴J. A. C. Veerman and D. Frenkel, *Phys. Rev. A* **45**, 5632 (1992).
- ³⁵M. Rigby, *Mol. Phys.* **66**, 1261 (1989).
- ³⁶A. Samborski and G. T. Evans, *J. Chem. Phys.* **101**, 6005 (1994).
- ³⁷E. Kierlik and M. L. Rosinberg, *Phys. Rev. A* **44**, 5025 (1991).
- ³⁸H. Zhong and R. Petschek, *Phys. Rev. E* **51**, 2263 (1995).
- ³⁹T. Boublík, *Mol. Phys.* **27**, 1415 (1974).